Journal of Organometallic Chemistry, 332 (1987) 35–46
Elsevier Sequoia S.A., Lausanne – Printed in The Netherlands

Coordinative interactions in chelated complexes of silicon

XIV *. Regular or irregular exchange mechanisms in pentacoordinate silicon compounds: an interpretation based on crystal structures, DNMR-data and molecular modelling

Gerhard Klebe

Hauptlaboratorium, BASF Aktiengesellschaft, D-6700 Ludwigshafen (Federal Republic of Germany)

(Received January 8th, 1987)

Abstract

A crystal structure determination on 1-(2-(difluoromethylsilyl))-*N*,*N*-dimethylmethanamine (Ib) has revealed a strongly distorted trigonal bipyramidal coordination with N and F at apical positions. A coordinative interaction of 2.346(3) Å is present. Dynamic NMR-data for this complex and related pentacoordinated compounds indicate positional exchange of substituents at silicon with an energy barrier of 7–19 kcal/mol. For the exchange mechanism, regular (pseudorotation, turnstile rotation) and irregular processes, with bond rupture/bond reformation, are discussed. A computer simulation (MNDO-calculations) of the exchange process in 2-((methyl(trifluorosilyl)amino)methyl)pyridine (IIIa), which shows trigonal bipyramidal structure in the crystal and fluxional properties in solution, indicates that any distinction between the mechanisms is unreasonable and can be reduced to the question of which limiting Si–N distance can be regarded as still corresponding to a chemical bond. There is good agreement between the calculated and observed energy barriers. The structure correlation method is used to compare the calculated molecular transformation route with the Berry pseudorotation pathway.

Introduction

Extensive NMR-studies of coordination complexes with coordination states higher than four indicate fluxional behavior in solution [1,2]. For pentacoordination, regular and irregular exchange mechanisms of substituents at the central atom have been considered, mainly those derived from investigation of pentacoordinate phos-

* For part XIII see ref. 6g.

0022-328X/87/$03.50

phorous compounds [3]. The regular processes (Berry pseudorotation, turnstile rotation) occur with conservation of pentacoordination in all steps along the isomerization pathway, whereas the irregular positional exchange involves fission and reformation of one central atom to ligand bond; that is, there is an intermediate change of coordination number at the central atom.

Pentacoordinated silicon derivatives can be either cations, anions, or uncharged coordination complexes in which the valence shell expansion is achieved by Lewis acid base interaction. Crystal structure determinations have shown that these coordinative bonds spread over the whole range between "normal single" bonds and "pure" van der Waals contacts [4]. For pentacoordinate silicon anions the positional exchange of substituents at Si is explained by regular isomerization (pseudorotation) [5]. For the pentavalent coordination complexes, however, both regular and irregular mechanisms are considered as competitive isomerization pathways [4,7]. In most of these neutral complexes one of the five bonds, namely the "coordinative bond", is sufficiently weak that an irregular isomerization pathway may compete with the regular process.

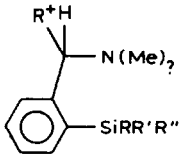

	R^+	R	R'	R"
Ia	H	F	F	F
Ib	H	Me	F	F
Ic	Me	F	F	F
Id	Me	Me	F	F

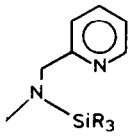

	R
IIIa	F
IIIb	Me

	R	R'	R"
IIa	F	F	F
IIb	Cl	Cl	Cl
IIc	Me	Cl	Cl
IId	Me	Me	Cl
IIe	Cl	F	F
IIf	Me	Me	Me

Corriu and his colleagues have intensively investigated the NMR properties of variously-substituted Si derivatives of benzylamines (Ia–Id) [6a,b] and dihydrogeno- and trihydrogeno-silanes derived from α-naphthylamine and (aminomethyl)-naphthaline [6c,d,e]. For all the compounds pentacoordination is assumed at low temperature. For Ia–Id the observed isomerization of substituents of silicon is explained in terms of pseudorotation which conserves pentacoordination along the pathway [6a]. For the naphthyl derivatives the NMR spectra are taken to indicate that for the trihydrogenosilanes pseudorotation is operative, but that this is not the case for the substituted dihydrogenosilanes [6c]. The crystal structures of two of the dihydrogenosilanes reveal markedly extended coordinative bonds (2.66, 2.584 Å) and the bond angles around silicon may be regarded as a perturbed trigonal bipyramid distorted towards a tetrahedron [6e]. Derivatives of 1,2,3,4-tetrahydro-1,10-phenanthroline (IIa–IIf) and 2-(methylamino)methylpyridine (IIIa, IIIb) have been investigated by crystal structure determinations and by NMR spectroscopy in solution [4,6f,g,7]. The crystal structure of IIa–IId,IIf reveals TBP geometry around Si. The central atom is bonded in the equatorial plane to the amino-type nitrogen. A Si...N coordinative bond, axial with respect to silicon, is formed by intramolecular Lewis acid base interaction to the pyridine-type nitrogen. The elongation of the coordinative bond amounts to 13–16% (IIa–IId, IIIa) with respect to a Si–N single bond. In IIf, where no halogen atom is present in the silyl group the Si...N bond is extended by 54%. In solution, dynamic NMR-studies (DNMR) revealed intramolec-

ular exchange of substituents at silicon for IIa, IIe, and IIIa, whereas for IIf and IIIb there was no evidence for pentacoordination even at −120 °C. The dynamic behavior was interpreted in terms of a bond rupture/bond reformation mechanism combined with the rotation of an intermediate four-coordinate silyl group.

The energy barriers were derived from DNMR-data by line shape analysis. For Ia the barrier (18.6(6) kcal/mol) is higher than for IIa and IIIa (7.5(2), 13.2(9) kcal/mol). For Ib which has a silyl substituent of lower Lewis acidity, there is a barrier of (13.3(2) kcal/mol) comparable to that for IIIa. Because of the lack of crystal data for Ia–Id, any explanation of these findings in terms of stronger coordinative interactions which influence the energy barrier of the exchange process was purely speculative, and in order to clarify whether the benzylamine derivatives I show stronger coordinative interactions than II or III, as evidenced by a shorter Si...N distance, the crystal structure of Ib was determined.

Experimental

Owing to their sensitivity to moisture, the crystals, grown from the pure compound by slow cooling from 60 °C to room temperature, were sealed in glass capillaries. The space group was shown on the CAD 4 diffractometer to be $P2_1/n$. The lattice constants were refined from the angular settings of 25 strong reflections: a 9.037(4), b 10.278(5), c 12.940(3) Å, β 107.02(3)°, $Z = 4$, V 1149(1) Å^3. Data were collected at room temperature up to $\sin \vartheta/\lambda$ 0.48 Å^{-1} with graphite monochromated Mo-K_α radiation in ω-scan mode, resulting in 1299 reflections. Three standard reflections were monitored at regular intervals (5600 s) and indicated a continuous decrease in diffraction power of 0.46% per hour; correction was made for this by applying a linear scale factor depending on the reflection serial number. After application of background correction (SDP system [8]) and averaging symmetry equivalent observations, 1074 unique reflections remained for structure solution.

The structure was solved by direct methods using Multan [9]. The refinement by least-squares procedures led to a final $R(F) = 0.069$, with anisotropic temperature factors for all non-hydrogen atoms. The positional parameters of the H atoms at the aromatic ring were taken from a difference Fourier whereas the hydrogen atoms on the benzyl-C were placed at calculated positions. A fixed overall temperature factor was applied to all H atoms. All refinements were performed with the SDP system [8].

Discussion of the crystal structure

The fractional coordinates of the atoms in Ib, the interatomic distances (in Å) and bond angles (°) are shown in Tables 1, 2 and 3, with the numbering scheme shown in Fig. 1.

Surprisingly the distance between Si and N is 2.356(3) Å, a rather large value, indicating a weak coordinative interaction. As in the comparable compounds IIa–IId, IIIa, and other complexes with benzylamine as ligand [10], the coordinated N occupies an axial position. Owing to the long and weak Si–N bond the geometry at Si is strongly distorted. Based on the angles around Si, the polyhedron can be described as an intermediate between a TBP and a tetrahedron. The Si is displaced

Table 1

Fractional coordinates and the isotropic equivalent of the thermal parameters (see above) of Ib, with estimated standard deviations in parentheses

Atom	x	y	z	$B(\text{Å}^2)$ [a]
Si	0.5647(2)	0.2732(2)	0.3087(1)	5.80(5)
F(1)	0.6235(5)	0.4159(4)	0.3584(3)	9.9(1)
F(2)	0.4996(5)	0.3205(3)	0.1868(3)	8.1(1)
N	0.4513(5)	0.0776(4)	0.2308(3)	4.8(1)
C(1)	0.4187(6)	0.2452(5)	0.3809(4)	4.3(1)
C(2)	0.2964(6)	0.1602(6)	0.3375(4)	5.0(1)
C(3)	0.1874(7)	0.1343(6)	0.3898(5)	6.8(2)
C(4)	0.1958(7)	0.1971(6)	0.4847(5)	7.4(2)
C(5)	0.3136(8)	0.2822(6)	0.5283(4)	7.1(2)
C(6)	0.4211(7)	0.3078(5)	0.4756(4)	5.7(2)
C(7)	0.2928(7)	0.0987(6)	0.2308(5)	6.7(2)
C(8)	0.5071(8)	−0.0370(6)	0.2987(5)	7.9(2)
C(9)	0.4637(8)	0.0493(7)	0.1237(5)	8.1(2)
C(10)	0.2596(7)	0.3106(7)	0.8365(6)	8.3(2)
H(3)	0.1020	0.0754	0.3564	*
H(4)	0.1203	0.1800	0.5260	*
H(5)	0.3173	0.3358	0.5958	*
H(6)	0.5055	0.3703	0.5071	*
H(71)	0.2391	0.1559	0.1704	*
H(72)	0.2324	0.0185	0.2185	*

[a] Starred atoms were refined isotropically, using an overall temperature factor. Anisotropically refined atoms are given in the form of the isotropic equivalent thermal parameter defined as:
$(4/3)^* [a^{2*} B_{1,1} + b^{2*} B_{2,2} + c^{2*} B_{3,3} + ab(\cos \gamma)^* B_{1,2} + ac(\cos \beta)^* B_{1,3} + bc(\cos \alpha)^* B_{2,3}]$

by 0.24 Å towards F(1) from the plane through F(2), C(1) and C(10). The two Si–C bond lenghts are closer to the usual values in tetravalent than in pentavalent derivatives [4].

Table 2

Distances (Å) in Ib, e.s.d. in parentheses

Si–F(1)	1.627(2)
Si–F(2)	1.590(2)
Si–N	2.346(3)
Si–C(1)	1.848(4)
Si–C(10)	1.899(4)
N–C(7)	1.448(5)
N–C(8)	1.467(5)
N–C(9)	1.453(4)
C(1)–C(2)	1.391(5)
C(1)–C(6)	1.379(5)
C(2)–C(3)	1.375(5)
C(2)–C(7)	1.510(5)
C(3)–C(4)	1.370(6)
C(4)–C(5)	1.365(6)
C(5)–C(6)	1.366(6)

Table 3

Angles (°) in Ib, e.s.d. in parantheses

F(1)–Si–F(2)	95.7(1)
F(1)–Si–N	173.5(2)
F(1)–Si–C(1)	98.1(2)
F(1)–Si–C(10)	99.0(2)
F(2)–Si–N	81.2(1)
F(2)–Si–C(1)	116.0(2)
F(2)–Si–C(10)	112.3(2)
N–Si–C(1)	78.3(1)
N–Si–C(10)	87.5(2)
C(1)–Si–C(10)	126.4(2)
Si–C(1)–C(2)	119.6(3)
Si–C(1)–C(6)	123.3(3)
C(1)–C(2)–C(3)	121.5(3)
C(2)–C(3)–C(4)	119.4(4)
C(3)–C(4)–C(5)	120.3(4)
C(4)–C(5)–C(6)	120.0(4)
C(5)–C(6)–C(1)	121.7(4)
C(1)–C(2)–C(7)	115.7(4)
C(2)–C(7)–N	107.8(3)
C(7)–N–C(8)	106.7(3)
C(7)–N–C(9)	112.5(3)
C(8)–N–C(9)	107.6(3)

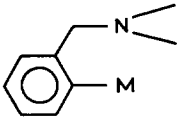

(IV)

The N is distorted by 0.50 Å out of a plane through its three neighbouring atoms, clearly indicating coordinative interaction to Si. A search through the Cambridge Crystallographic Data File revealed 87 independent fragments containing the fragment IV [11]. In these derivatives the N deviates from the plane through its next neighbours by between 0 and 0.58 Å.

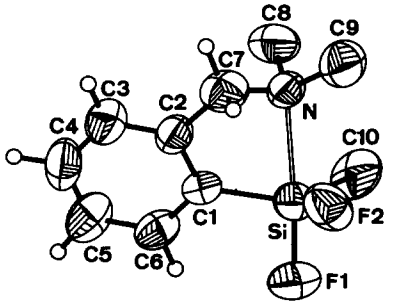

Fig. 1. Ortep drawing of the molecular structure of Ib. The thermal ellipsoids are the 50% probability surface with the H-atoms as spheres of arbirary size.

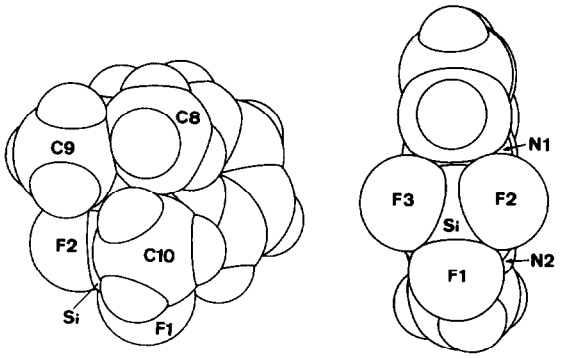

Fig. 2. Space filling model of Ib and IIIa, indicating close van der Waals contacts between various atoms in the molecules.

It is usually assumed that an aliphatic nitrogen (as in Ib) is more nucleophilic and hence stronger as a Lewis base than an aromatic N (as in IIIa N(2)), but the coordinative bond is much longer in Ib than in IIIa (1.974(6) Å). It is necessary to consider factors which could give rise to the bond lengthening. Because of the geometry of the ligand, it was conceivable that a shorter Si–N contact could only be achieved at the cost of considerable strain, but this explanation is ruled out by the observation that a nickel complex with the same ligand [12] shows two Ni–N distances of 1.973 and 1.976 Å respectively. As Si and N both bear bulky methyl groups, it is necessary to consider whether steric hindrance between these substituents prevents a shorter Si...N contact. A space filling model of Ib (Fig. 2) shows, that the van der Waals surfaces of the substituents under consideration are rather close. However, a shortening of the Si–N distance could also be achieved, by a more marked pyramidalization at N (see above) and a smaller deviation of Si from the basal plane. This shortening should not lead to an increasing steric interaction between the methyl groups in the complex. In the Ni complex and in IIIa (see Fig. 2) the molecular framework allows a staggered arrangement of the ligand and the substituents at the central atom, which avoids short van der Waals contacts. However, steric crowding in Ib may be the explanation of the longer bond in Ib compared with that in IIIa. Furthermore, there may be some intermolecular forces which compete with and affect the intramolecular Si–N interaction, but a close examination of the packing in the unit cell of Ib does not provide evidence in favour of this possibility.

Discussion and simulation of the exchange pathway

The dynamic exchange mechanism must be re-discussed in the light of the molecular structures.

The coordinative Si–N bond in Ib is much longer and hence weaker than in IIa–IId and IIIa (IIa: 1.969(4), IIb: 1.984(2), IIc: 2.027(4), IId: 2.028(7), IIIa: 1.974(6) Å [6f,7a,b]. It is midway between those in the halogen-containing compounds IIa–IId,IIIa and those in the $SiMe_3$ complex IIe (2.689(8) Å [4]) and the two dihydrogenosilanes [6e] (2.66, 2.584 Å). As mentioned earlier, the energy barrier for the positional exchange of substituents at Si derived for Ib from DNMR-data is very close to that for IIIa [6f]. Hence there cannot be a simple correlation between

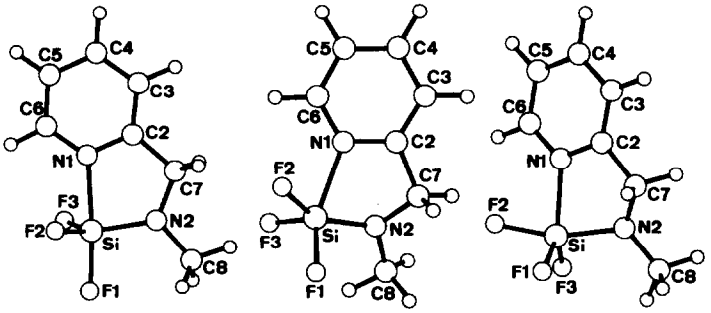

Fig. 3. Computed molecular structure of IIIc along the isomerization pathway. The torsion angle τ is that between C(7)–N(2)–Si–F(2), left: TBP-like geometry related to the crystal structure τ −83°, center: intermediate geometry τ 7°, right TBP-like geometry with F(2), N(2) apical τ 37°.

increasing coordinative interaction and the height of energy barrier. Any interpretation of the dynamic properties and any conclusions about the activation barrier in solution requires detailed information on the molecular geometry. In the processes involved, various effects can contribute to the total energy barrier. Besides the coordinative Si–N interaction, the steric crowding in the ligand and its potential flexibility, and the partial double bond character of the bond between Si and the pivot atom [6g] are aspects which must be considered.

From the NMR-data, fluxional behaviour is evident for derivatives I, II, and III. Both, regular and irregular processes were considered for the intramolecular positional exchange of substituents at silicon. The distinction between the two mechanisms involves the question of whether the central atom remains pentavalent throughout the whole process or whether its bonding geometry is so strongly distorted that one of its linkages is broken (expanded beyond the bond-limit); in this case there is an intermediate, in which the coordination at Si is four.

Quantum mechanical calculations on the pathway were performed in order to cast some light on the detailed molecular motions during the dynamic exchange process. Ab initio calculations require much computing time for a molecule of this size and so semi-empirical MNDO calculations [13] were performed. Compound IIIa was chosen, and the calculations were based on the geometry in the crystal [6f,14*]. The torsion angle C(7)–N(2)–Si–F(2) (labeling scheme see Fig. 3) was varied in steps of 10° to simulate a rotation of the SiF_3 group ($\Delta\tau$ 120°). The geometry was optimized at each point along the isomerization pathway [15]*].

The procedure may seem to imply simulation of an irregular isomerization pathway only, but since MNDO calculations do not require any information about the connections between atoms, no constraint is imposed on the valency at silicon.

In Tables 4 and 5 the calculated energy and the distances and angles at silicon are listed for each step. The TBP-like starting geometry (τ −83°) with N(1) and F(1) apical (cf. crystal structure), an intermediate (τ 7°) and the "final" TBP-like geometry with N(2) and F(2) apical (τ 37°) are shown in Fig. 3. Calculations beyond τ 37° reveal geometrical changes at Si which are similar to those between τ −83° and 37°.

* This and other references marked with asterisks indicate notes occurring in the list of references.

Table 4

Calculated energy (kcal) and selected distances (Å) in the computed arrangements of IIIa along the isomerization pathway. The reaction coordinate is specified by the torsion angle τ (C(7)–N(2)–Si–F(2)). The last line (XS) lists the corresponding distances in the crystal structure

Coordinate (C(7)–N(2)–Si–F(2))	E	Si–N(1)	Si–N(2)	Si–F(1)	Si–F(2)	Si–F(3)
−83	0.16	2.080	1.791	1.658	1.654	1.654
−73	0.33	2.089	1.791	1.657	1.655	1.653
−63	0.36	2.083	1.792	1.658	1.656	1.652
−53	0.00	2.090	1.790	1.658	1.654	1.651
−43	0.35	2.103	1.790	1.657	1.655	1.648
−33	1.19	2.128	1.788	1.655	1.655	1.645
−23	2.45	2.148	1.789	1.654	1.656	1.644
−13	4.05	2.174	1.793	1.652	1.654	1.642
−3	6.30	2.195	1.796	1.650	1.654	1.641
7	8.32	2.112	1.818	1.654	1.663	1.642
17	9.61	2.102	1.823	1.653	1.665	1.643
27	10.30	2.055	1.837	1.654	1.668	1.647
37	10.46	2.038	1.842	1.653	1.671	1.650
XS −83		1.973	1.704	1.621	1.603	1.603

The evaluation of the geometrical changes along the isomerization pathway assisted by computer graphics [16*] shows that the distance between Si and the pyridine-type N increases relative to that for TBP geometry in the crystal structure, indicating that the weakest interaction is probably easily lengthened to allow a preferred transition pathway. However, it never becomes longer than 2.2 Å. The skeleton of the ligand follows the rotation of the silyl group in a way that could be related to the molecular motions corresponding to rearrangement along the Berry or turnstile coordinate (see Fig. 3, Tables 4, 5). Which of the two limiting mechanisms, regular or irregular, should these computer simulations be associated with? Taking them as an indication of how positional exchange in IIIa occurs in solution, any distinction between a regular and irregular pathway appears to be unjustified and unreal. In view of the large range of Si–N distances observed in crystal structures [4] and the lengthening of the Si–N distance indicated by the present calculations, the distinction between regular and irregular mechanisms can only be maintained if a distance limit is specified beyond which a Si–N contact is no longer regarded as a bond. Such a limit must be arbitrary, and chemically meaningless. This argument appears to be even more relevant for complexes such as Ib (cf. NMR studies [6a]), where the crystal conformation shows a longer Si–N contact than any distance found along the simulated pathway for IIIa. For the present type of coordination complexes it seems reasonable that with decreasing strength of the coordinative bond (indicated by its length in the crystal conformation) this linkage becomes more and more readily distorted and extended during the isomerization process (thus resembling more and more the geometrical requirements of an irregular process). Of course, it is necessary to consider how reliable and valid the computer simulations are. In the present study the calculated energy barrier (10.5 kcal) is close to the $\Delta H^{\ddagger}$ derived from NMR experiments (13.2(9) kcal/mol). It is not clear whether the agreement indicates an excellent simulation of the pathway or is rather accidental,

Table 5

Angles around silicon in the computed arrangements of IIIa along the isomerization pathway. The reaction coordinate is specified by the torsion angle τ (C(7)–N(2)–Si–F(2)). The last row (XS) shows the corresponding angles in the crystal structure

Coordinate (C(7)–N(2)–Si–F(2))	N(1)–Si–N(2)	N(1)–Si–F(1)	N(1)–Si–F(2)	N(1)–Si–F(3)	N(2)–Si–F(1)	N(2)–Si–F(2)	N(2)–Si–F(3)	F(1)–Si–F(2)	F(1)–Si–F(3)	F(2)–Si–F(3)
−83	83.21	175.18	83.71	83.56	101.61	119.74	120.07	93.92	93.79	116.38
−73	82.75	175.29	82.87	84.29	101.87	120.51	119.56	93.88	94.14	115.89
−63	82.54	175.42	82.18	85.39	101.28	121.17	119.25	93.62	94.83	115.61
−53	81.87	175.93	82.40	85.59	101.38	121.89	118.80	93.75	94.89	115.20
−43	80.49	175.18	81.27	87.05	101.18	123.73	117.93	94.09	96.06	113.67
−33	78.96	174.29	80.15	87.86	101.23	125.66	116.79	95.28	97.06	111.86
−23	77.57	170.40	78.70	89.97	101.34	129.37	115.05	95.11	99.04	108.96
−13	76.00	167.60	77.97	91.39	101.61	132.07	112.89	95.49	100.66	107.25
−3	74.61	162.22	76.50	95.15	101.83	135.53	110.75	95.60	102.31	104.83
7	76.36	148.74	78.80	104.69	98.46	148.94	104.93	93.16	106.41	99.14
17	76.36	141.94	79.29	109.06	98.73	152.62	102.91	92.72	108.81	96.70
27	78.10	133.33	81.67	115.39	97.20	158.95	99.78	92.42	111.18	94.08
37	79.94	124.75	82.67	121.14	97.25	162.60	97.52	92.62	113.97	91.46
XS − 83	86.82	178.05	86.08	86.08	91.23	125.22	125.22	95.05	95.05	108.33

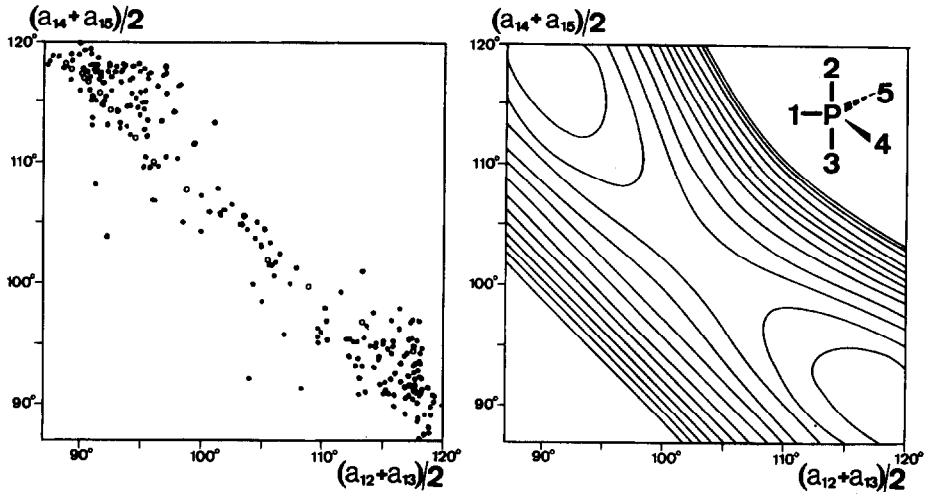

Fig. 4. Correlation of experimentally determined pentavalent P-structures (●) and calculated arrangements for Ib (○) along the Berry pathway (left). Potential energy surface for PF_5, computed by MNDO; contour interval 1 kcal (right).

but in any case the present results indicate that mechanistic explanations in terms of limiting mechanisms are sometimes insufficient and misleading.

As indicated in Tables 4 and 5 the energy varies only a little during the first five steps along the pathway. Accordingly the geometry in the coordination sphere around silicon remains nearly unchanged. Along these incipient steps the molecular motions are mainly due to pseudorotation of the five-membered heterocycle.

In agreement with the crystal data the MNDO calculations reveal a planar arrangement around the amino-type nitrogen N(2) in the equatorial position (τ $-83°$), whereas there is pyramidalization at N(2) when it is in the apical site (τ $37°$). These differences could indicate different bonding properties for Si–N linkages at the equatorial or axial positions owing to an anisotropic charge distribution in this bond. This assumption is supported by the fact that electron density studies on IIb [6g] revealed the lone pair at the trigonal planar N (on the equatorial site) to be significantly displaced towards silicon. This effect leads to an non-axial-symmetric charge distribution in the Si–N bond (cf. d_π–p_π bonding).

As mentioned previously the ligand skeleton follows the rotation of the silyl group in a way expected for the Berry pseudorotation or turnstile rotation. The angles of the intermediate (τ $7°$) are closer to those in the transition state structure of the Berry pseudorotation than to those for the turnstile rotation [17]. These findings are supported by the structure correlation shown in Fig. 4, where crystal and electron diffraction data (●) for pentavalent P compounds [11,18] are correlated and plotted together with the computed data (○).

In order to correlate the coordination geometry around P in the various crystal structures with the C_{2v}-symmetrical Berry pathway the arithmetic means of the angles between the pivot atom and two ligand atoms in each of the perpendicular mirror planes were used [19]. The computed valence angle changes in IIIa fit nicely at the center of the data sample.

Bürgi and Dunitz [19] mentioned the attractive idea that the sample points of such a structure correlation tend to congregate in the low-lying region of the potential energy surface which underlies the idealized pathway under consideration, e.g. the positional exchange of fluorine in PF_5. To derive a corresponding potential energy surface for PF_5 the above defined angles (reaction coordinates) were systematically varied within the scope of the experimental data (Fig. 4) and the energy was computed by the MNDO method. The calculated values were contoured with an interval of 1 kcal/contour. As a comparison with ab initio calculations for the Berry pseudorotation of PF_5 shows, the energy is resonably well reproduced by MNDO [20] (the energy difference between the trigonal bipyramid and the square pyramid amounts to 4.95 kcal (ab initio) and 4.8 kcal (MNDO) respectively). The experimentally observed arrangements around P correspond to the low-lying region of the pontential energy surface of the idealized process derived for the PF_5 molecule.

Supplementary material available. Listing of anisotropic temperature factors and the observed and calculated structure factors are available through the Fachinformationszentrum Energie-Physik-Mathematik, D-7514 Eggenstein-Leopoldshafen, under the deposit number CSD-52266, together with the journal reference. A list of the Refcodes of the crystal structures and the references for the electron diffraction data used in Fig. 4 has also been deposited.

Acknowledgement

The author thanks Prof. R.J.P. Corriu (Univ. Montpellier, France) for a sample of Ib, and Prof. H. Fuess and the Institut für Kristallographie and Mineralogie (Univ. Frankfurt/M., Fed. Rep. Germany) for making the diffractometer available.

References

1 D.L. Kepert, Inorg. Stereochemistry, Springer Verlag, 1982.
2 M.G.B. Drew, Coord. Chem. Rev., 24 (1977) 179.
3 R. Holmes, Pentacoordinated Phosphorus, Am. Chem. Soc., Washington DC., Vols. 1 and 2, 1980, and ref. therein.
4 G. Klebe, J. Organomet. Chem., 293 (1985) 147.
5 a. W.H. Stevenson and J.C. Martin, J. Am. Chem. Soc., 104 (1982) 309.
5 b. F. Klangberg and E.L. Muetterties, Inorg. Chem., 7 (1968) 155.
5 c. J.A. Gibson, D.G. Ibbott and A.J. Janzen, Can. J. Chem., 51 (1973) 3203.
5 d. W.G. Farnham and R.L. Harlow, J. Am. Chem. Soc., 103 (1981) 4608.
6 a. R.J.P. Corriu, A. Kpoton, M. Poirier, G. Royo and J.Y. Corey, J. Organomet. Chem., 277 (1984) C25.
6 b. R.J.P. Corriu, G. Royo and M. Poirier, J. Organomet. Chem., 233 (1982) 165.
6 c. J. Boyer, R.J.P. Corriu, A. Kpoton, M. Mazhar, M. Poirier and G. Royo, J. Organomet. Chem., 301 (1986) 131.
6 d. R.J.P. Corriu, M. Mazhar, M. Poirier and G. Royo, J. Organomet. Chem., 306 (1986) C5.
6 e. C. Breliere, F. Carre, R.J.P. Corriu, M. Poirier and G. Royo, Organometallics, 5 (1986) 388.
6 f. G. Klebe, M. Nix and K. Hensen, Chem. Ber., 117 (1984) 797.
6 g. G. Klebe, J.W. Bats and H. Fuess, J. Am. Chem. Soc., 106 (1984) 5202.
7 a. G. Klebe, J.W. Bats and K. Hensen, J. Chem. Soc., Dalton Trans., (1985) 1.
7 b. G. Klebe, K. Hensen and H. Fuess, Chem. Ber., 116 (1983) 3125.
7 c. G. Klebe, K. Hensen, J. Chem. Soc., Dalton Trans., (1985) 5.
7 d. G. Klebe, K. Hensen and J. v. Jouanne, J. Organomet. Chem., 258 (1983) 137.

8 B.A. Frenz, Structure Determination Package (SDP) Program System, Enraf-Nonius, Delft, The Netherlands, 1982.
9 P. Main, L. Lessinger, M.M. Woolfson, G. Germain and J.P. Declerg, Multan a Computer Program for the Automatic Solution of Crystal Structures, Univ. of York, 1980.
10 a. C. Breliere, F. Carre, R.J.P. Corriu, A. De Saxce, M. Poirier and G. Royo, J. Organomet. Chem., 205 (1981) C1.
10 b. G. v. Koten, J.G. Noltes and A.L. Spek, J. Organomet. Chem., 118 (1976) 183.
11 Cambridge Structural Database System, Vers. 2. CPS, Cambridge Crystallographic Data Center, Univ. Chemical Laboratory, Lensfield Road, Cambridge, 1985.
12 D.M. Grove, G. v. Koten, H.J.C. Udbels, R. Zoet and A.L. Spek, J. Organomet. Chem., 263 (1984) C10.
13 J.J.P. Stewart, MOPAC,QCPE-Program No. 455, Indiana Univ., Bloomington, USA, 1985.
14 The molecular geometry derived from the crystal structure of IIIa was taken as the starting conformation for a full MNDO-optimization. The optimized structure agrees reasonably well (Tab. 4, 5) with the crystal conformation. Any MNDO-simulation based on the crystal structure of Ib leads to marked lengthening of the coordinative bond, so that the crystal geometry is not satisfactorily reproduced.
15 In order to test the results, the calculations along the pathway were performed in both directions leading to the same geometrical transformations.
16 a. Chem-X, developed and distributed by Chemical Design Ltd., Oxford, England.
16 b. Sybyl, developed and distributed by Tripos Associates, Inc., St. Louis, Missouri, USA.
17 P. Narayanan, H.M. Berman, F. Ramirez, J.F. Marecek, Y. Chaw and V.A.V. Prasad, J. Am. Chem. Soc., 99, (1977) 3336.
18 I. Buck, E. Maier, R. Mutter, U. Seiter, C. Spreter, B. Strack, I. Hargittai, O. Kennard, D.G. Watson, A. Lohr, T. Pirzadeh, H.G. Schirdewahn and Z. Majer; Bibliography of Gas Phase Electron Diffraction 1930–1979, Physics Data No. 21-1, Fachinformationszentrum, Karlsruhe, 1981.
19 H.B. Bürgi and J.D. Dunitz, Acc. Chem. Res., 16 (1983) 153.
20 C.J. Marsden, J. Chem. Soc., Chem. Comm., (1984) 401.